



## Sea-ice motion and oceanographic data from the Beaufort Sea to the Chukchi Borderland in March–October 2022

Satoshi KIMURA<sup>1\*</sup>, Takashi KIKUCHI<sup>1</sup>, Amane FUJIWARA<sup>1</sup>, Joshua JONES<sup>2</sup>,  
Masahiro KAKU<sup>1</sup>, and Kensuke WATARI<sup>1</sup>

<sup>1</sup> Japan Agency for Marine-Earth Science and Technology, 2-15, Natsusima-cho,  
Yokosuka, Kanagawa 237-0061.

<sup>2</sup> Geophysical Institute University of Alaska Fairbanks, 2156 Koyukuk Drive,  
University of Alaska Fairbanks, Fairbanks, AK 99775.

\*Corresponding author. Satoshi Kimura ([skimura@jamstec.go.jp](mailto:skimura@jamstec.go.jp))

(Received March 17, 2023; Accepted June 2, 2023)

**Abstract:** The Pacific sector of the Arctic Ocean is experiencing sea-ice reduction, yet there are not many ocean observations beneath sea ice. We present oceanographic observations within 18 m of sea ice with 4 CTDs, phytoplankton biomass, and photosynthesis available radiation (PAR) from an ice-tethered buoy and surrounding sea-ice motions from 10 GPS buoys in the Beaufort Sea.

### 1. Background and Summary

Summertime sea-ice reduction in the Siberian Shelves and the Canada Basin is one of the significant components of the declining sea-ice area in the Arctic Ocean. Two factors thought to be responsible for the sea-ice reduction are 1) increasing heat transport from the Pacific (Woodgate *et al.* 2012)<sup>1</sup> and 2) ice-albedo feedback processes, which increase the surface melting of sea ice (Perovich *et al.* 2007<sup>2</sup>; Kashiwase *et al.* 2017<sup>3</sup>).

The freshwater inputs from increasing sea-ice melt and the river runoff have accumulated in the center of the anticyclonic Beaufort Gyre (Proshutinsky *et al.* 2009)<sup>4</sup>. The accumulated freshwater has a 30-year 0.11–0.19 PSU/yr trend toward a fresher surface layer in the Canada Basin (Peralta-Ferriz and Woodgate 2015)<sup>5</sup>. The freshening stabilizes the surface-mixed layer, which can change the transfer of heat between ocean, sea ice, and atmosphere (Sirevaag *et al.* 2011<sup>6</sup>; Steele *et al.* 2011<sup>7</sup>); melting/freezing cycle of sea ice (Polyakov *et al.* 2013<sup>8</sup>; Shimada *et al.* 2006<sup>9</sup>); and the vertical transport of nutrients (Carmack *et al.* 2015)<sup>10</sup>. However, the freshening trend of the surface mixed layer in the Arctic Ocean remains

underrepresented in climate models (Rosenblum *et al.* 2021)<sup>11</sup>. As the summertime surface-mixed layer depth can be shallower than the vertical resolution in climate models (~10 m), there is a need to quantify the mechanism of the freshwater discharge from sea ice. Here, we present GPS data to track the sea-ice motions and the ocean dynamics beneath the ice with 4 CTD sensors, building on our previous study, which only employed 1 CTD during the ICEX 2020 (Kimura *et al.* 2021)<sup>12</sup>.

## 2. Observation Site

A total of 10 GPS buoys and one ice-tethered Warming and Irradiance Measuring (WARM) buoy (Table 1) were deployed approximately 200 km northeast of Prudhoe Bay, Alaska on drifting sea ice during the ICEX 2022 exercise, hosted by the U.S. Navy, in March 2022. Our observations extend from the Beaufort Sea to the east of the Chukchi Borderland in March–November 2022 (Figure 1). The ice-tethered buoy drifts westward to the Chukchi Borderland from the deployment site along the continental shelf, a similar flow pattern to the buoy deployed in ICEX 2020. However, the buoy track in 2022 is different once it reaches the Chukchi Borderland. The track in 2022 follows the eastern side of the Chukchi Borderland and heads northward, while the track in 2020 flows on the south side into the Chukchi Sea. The track in 2022 becomes closer to the two buoys operated by the Ice Tethered Platform (ITP) program led by Wood Hole Oceanographic Institution. The tracks of ITP data are available at the ITP website (<https://www.whoi.edu/website/itp/overview>).

## 3. Methods

### Buoy Design

Five “Universal Tracker” (UT) GPS buoys (JAM-UT-0006–JAM-UT-0010) and “Ice Tracker” (IT) GPS buoys (JAM-IT-0006–JAM-IT-0010) were placed with the ice-tethered WARM buoy, JAM-WB-0004. These GPS buoys monitor the deformation of sea-ice floes around the ice-tethered buoy. The 5 UT and 5 IT buoys are initially positioned within ~500 m and ~10 km from the ice-tethered buoy, which permits us to quantify the sea-ice deformation in two different spatial scales (Figure 2). We deployed JAM-WB-0004 on March 17, 2022. The data is presented starting March 20. The Ice Tracker, Universal Tracker, and WARM buoy are off-the-shelf commercial products, which is engineered by Pacific Gyre Inc. (<https://www.pacificgyre.com>). The GPS accuracy is the GPS standard of 3.5 meters.

The ice-tethered buoy JAM-WB-0004 consists of 4 CTDs, 2 PAR sensors (Licor L1-192), and 2 chlorophyll sensors (Figure 3). The CTDs are JES10mini, manufactured by Offshore Technologies (<https://www.offshore-technologies.com/en/products/>). The chlorophyll sensors are manufactured by Sea-Bird Scientific (<https://www.seabird.com/>). This compact, lightweight CTD offers to refine the vertical

sample resolution. We refer to them as sensors 2, 4, 5, and 6, initially located at 2, 4.8, 12.8, and 15.6 dbar, respectively. Sensor 3 was placed between sensors 2 and 4, but it failed after 9 days. In addition to CTDs, we monitor phytoplankton biomass and its response to light intensity. The buoy is equipped with two chlorophyll sensors and PAR sensors. The GPS positions, temperature, salinity, and pressure are recorded every 30 minutes. We place the webcam Sidekick buoy (JAM-SK-0003) beside the ice-tethered buoy to take daily photos of the deployment site. The Sidekick is equipped with two cameras in front and back. The front camera takes the top of the ice-tethered buoy, and the back camera takes the surroundings.

#### 4. Data Overview and Validation

Data from JAM-WB-0004 were compared to data from the ITP. The tracks of ITP #131 and 136 are close to the track of JAM-WB-0004 from the end of September to October ([Figure 1](#)). Although the JAM-WB-0004 record contains many short time-scale fluctuations, the temperature decreases in time, which is a similar feature to the ITP measurements ([Figure 4a](#)). Sensor 2 detects a sudden salinity decrease on October 6, which is also present in the ITP #136 measurements ([Figure 4b](#)). Apart from this drop in salinity, both salinity measurements decrease over time.

One of the main differences between JAM-WB-0004 and the buoy deployed in 2020 is in the number of CTDs. Some of the CTDs are placed  $\sim 2$  m apart, and the uncertainties of the measurements may overlap when the distributions of temperature and salinity are uniform in the vertical direction. We quantify the inherent uncertainties in temperature and salinity measurements by employing the root mean square of the conductivity and temperature errors from the pre-deployment calibration done by the manufacturer ([Figure 4a, b](#)). The temperature uncertainties in sensors 2, 4, 5, and 6 are  $\pm 7.16 \times 10^{-5}$ ,  $\pm 6.88 \times 10^{-5}$ ,  $\pm 5.70 \times 10^{-5}$ ,  $\pm 9.16 \times 10^{-5}$  °C, respectively. Similarly, the salinity uncertainties in sensors 2, 4, 5, and 6 are  $\pm 0.0880$ ,  $\pm 0.117$ ,  $\pm 0.119$ , and  $\pm 0.11$  PSU, respectively. We can evaluate the uncertainties associated with the potential density anomaly  $\sigma_0$  with respect to a reference pressure of 0 dbar, based on these temperature and salinity uncertainties. We ensure that there is no prolonged density overturning within the uncertainties of the measurements ([Figure 4c](#)).

The salinity record from sensor 2 experienced a significant decrease starting from July 1. We assess this salinity drop by the pressure record and daily photos of the top buoy by JAM-SK-0003. The top buoy was pegged on the ice surface by ice screws, approximately 3 m away from the borehole, so the pressure from the CTD records should increase  $\sim 3$  dbar, when the ice screws are loosened by sea-ice weakening ([Figure 4d](#)). An equivalent level of pressure decrease is observed towards the end of September; however, we do not have photos to assess the cause. We speculate that the buoy is lifted by the sea-ice deformation. There is a decrease in the variability of temperature and salinity after the pressure decrease. The magnitudes of these variabilities appear to be similar during the period spanning from March to July,

wherein the CTD sensors remain positioned beneath the sea ice. Sensor 2 was likely frozen during April, May, and June (Figure 5). Salinity during the frozen period was nearly zero. The salinity signal came back to 28 PSU at the end of June when the surface was covered by water (Figure 6). JAM-WB-0004 appeared to be inside a melt pond. When salinity in sensor 2 dropped back to 0 on July 3, the melt pond had been drained (Figure 7). The temperature record from sensor 2 indicated warming from July 3, and almost reached the freezing point temperature of freshwater. We speculate from this chain of events that sensor 2 has been measuring a melt pond draining event on July 1.

The records of chlorophyll-a concentration showed a gradual increase toward May with a slight increase in solar irradiance and decreased by the end of June (Figures 4e, f). It suggests phytoplankton production consumed nutrients before sea ice break-up forming under-ice bloom ( $\sim 1.1 \mu\text{g L}^{-1}$  in maximum); however, our buoy did not capture massive phytoplankton bloom as in Hill *et al.*, (2018)<sup>13</sup>. The upper fluorometer record showed unrealistic small values from Jun 30, probably due to some mechanical problems and lost the signal from August 30. On the other hand, the lower fluorometer has continued to record post-bloom chlorophyll-a variability toward fall, capturing a weak fall bloom signal.

## 5. Data Records

The raw data have been organized into the 10 NetCDF (Network Common Data Form) files with filenames corresponding to the device names in Table 1. Each file contains latitude and longitude from the GPS with variable names, “Latitude” and “Longitude”. The sampling time is stored as variable names, “Year”, “Month”, “Day”, “Hour”, “Minute”, and “Second”. In addition to these variables, the ice-tethered buoy (OceanDATA\_JAM-WB-0004.nc) contains 4 sets of temperature, salinity, pressure, and the minimum and maximum possible temperature and salinity from the pre-deployment calibrations. The daily-mean chlorophyll and PAR are in a separate NETCDF file (OceanDailyMean.nc).

NetCDF is a machine-independent data format that supports the creation, access, and sharing of array-oriented scientific data through various programming interfaces. The details of the NetCDF format are given on the web manual page (<https://www.unidata.ucar.edu/software/netcdf/>).

We include daily photos of the deployment site from March 17–Sep 23, 2022, although our webcam Sidekick turns sideways on Aug 1. The images are in jpg format. The filename consists of the device name, date, and image number, e.g. “JAM-SK-0003\_2022-06-21\_00353.jpg”, where “JAM-SK-0003” is the device name, “2022-06-21” indicates June 21, 2022, the last digits represent the image number.

6. Figures

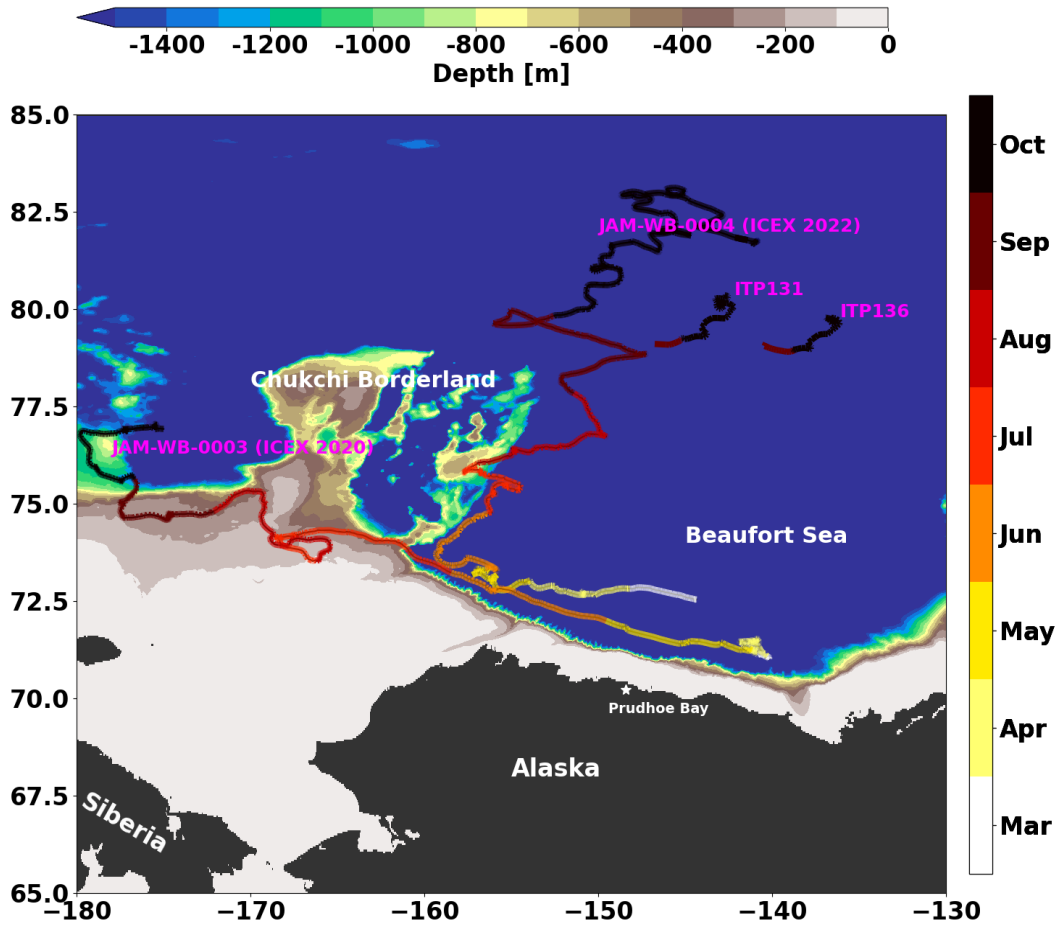


Figure 1. Buoy tracks in 2020 and 2022 from March to October. ITP131 and ITP136 are the ice-tethered profiler (ITP) data in 2022 by Woods Hole Oceanographic Institution. The JAM-WB-0003 is our buoy deployed on March 20, 2020, as a part of ICEX 2020.

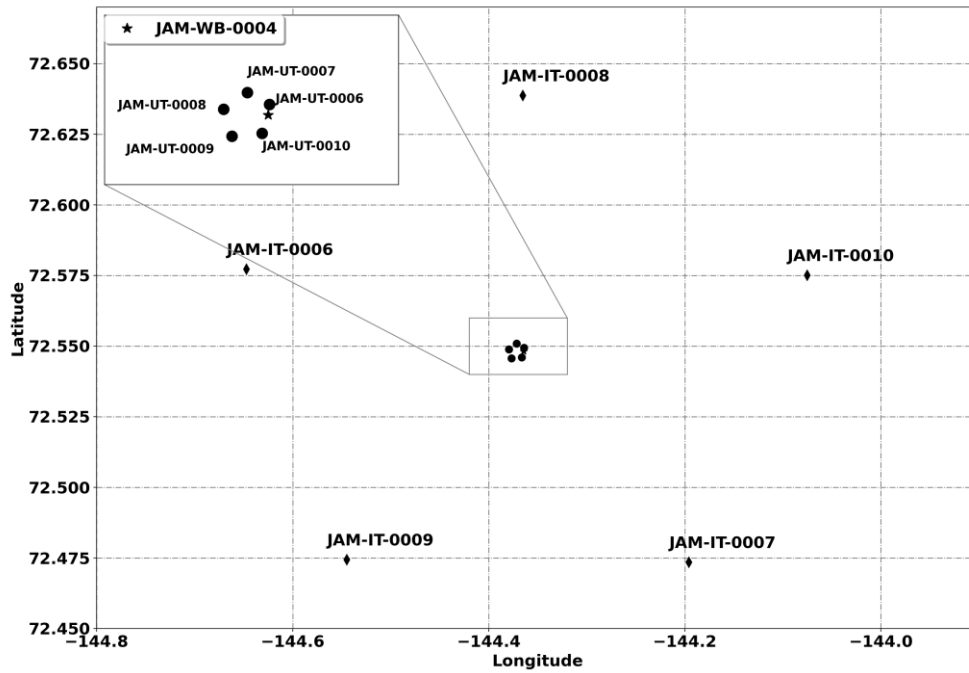


Figure 2. Initial positions of the ice-tethered buoy and GSP buoys on March 20, 2022. Latitude and longitude are displayed in decimal degrees.

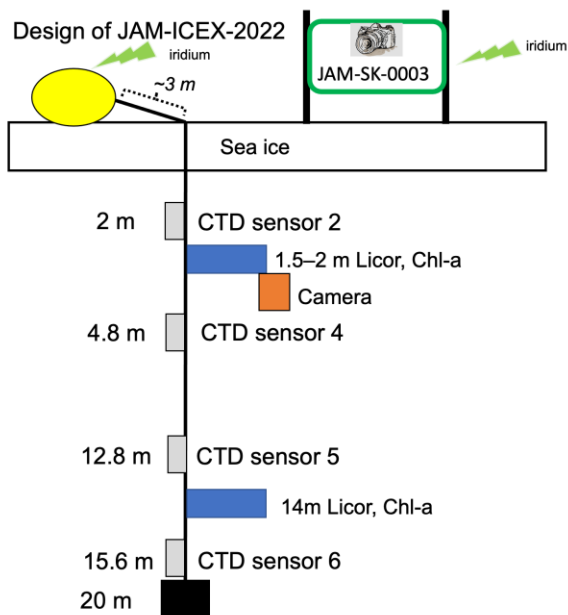


Figure 3. Buoy design. The depth in meter indicates the initial position of the instruments.

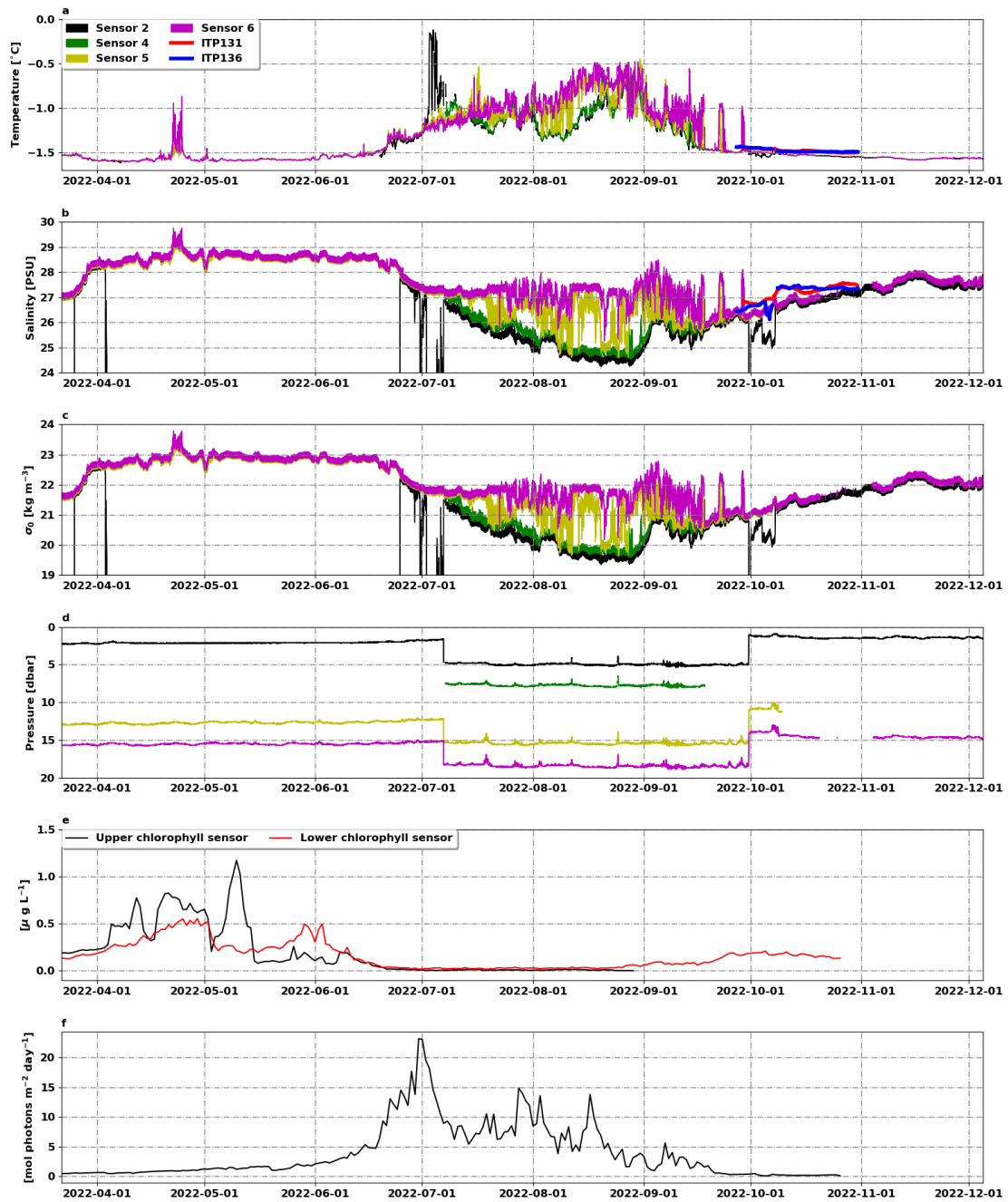


Figure 4. JAM-WB-0004 data from March 20–November 1, 2022, a) temperature, b) salinity, c)  $\sigma_0$ , d) pressure, e) chlorophyll, and f) PAR. The blue and red lines in (a) and (b) represent the daily-averaged ITP profiles above 20 dbar.



Figure 5. Overlooking JAM-WB-0004 on June 20 (JAM-SK-0003\_2022-06-20\_00352.jpg).



Figure 6. Overlooking JAM-WB-0004 on June 24 (JAM-SK-0003\_2022-06-24\_00360.jpg).



Figure 7. Overlooking JAM-WB-0004 on July 3 (JAM-SK-0003\_2022-07-03\_00378.jpg).

## 7. Table

Table 1. List of buoys.

Device name	Type	Data start date	Deployment location	Total duration (Days)	IMEI
JAM-WB-0004	Ice-tethered WARM buoy	March 20 2022	72.548, -144.364	258	300534062265120
JAM-UT-0006	GPS, Universal Tracker	March 20 2022	72.549, -144.364	183	300234066309170
JAM-UT-0007	GPS, Universal Tracker	March 20 2022	72.551, -144.372	202	300534062268790
JAM-UT-0008	GPS, Universal Tracker	March 20 2022	72.549, -144.38	175	300534062361400
JAM-UT-0009	GPS, Universal Tracker	March 20 2022	72.546, -144.377	202	300534062367380
JAM-UT-0010	GPS, Universal Tracker	March 20 2022	72.546, -144.366	191	300534062369380
JAM-IT-0006	GPS, Ice Tracker	March 20 2022	72.577, -144.647	226	300234064708300
JAM-IT-0007	GPS, Ice Tracker	March 20 2022	72.474, -144.196	220	300234066300590
JAM-IT-0008	GPS, Ice Tracker	March 20 2022	72.639, -144.365	226	300234066302180
JAM-IT-0009	GPS, Ice Tracker	March 20 2022	72.474, -144.545	226	300234066305010
JAM-IT-0010	GPS, Ice Tracker	March 20 2022	72.575, -144.075	226	300234066305080

## References

1. Woodgate, R. A, Weingartner, T. J. and Ron Lindsay. Observed increases in Bering Strait oceanic fluxes from the Pacific to the Arctic from 2001 to 2011 and their impacts on the Arctic Ocean water column. *Geophysical Research Letters*. 2012, 39 (24). <https://doi.org/10.1029/2012GL054092>.
2. Perovich, D. K, Light, B., Eicken, H., Jones, K. F., Runciman, K. and Nghiem, S. V. Increasing solar heating of the Arctic Ocean and adjacent seas, 1979–2005: Attribution and role in the ice-albedo feedback. *Geophysical Research Letters*. 2007, 34 (19). <https://doi.org/10.1029/2007GL031480>.
3. Kashiwase, H., Ohshima, K. I., Nihashi, S. and Eicken, H. Evidence for ice-ocean albedo feedback in the Arctic Ocean shifting to a seasonal ice zone. *Scientific Reports*. 2017, 7: 8170. <https://doi.org/10.1038/s41598-017-08467-z>.
4. Proshutinsky, A. et al. Beaufort Gyre freshwater reservoir: State and variability from observations. *Journal of Geophysical Research: Oceans*. 2009, 114 (C1). <https://doi.org/10.1029/2008JC005104>.
5. Peralta-Ferriz, C. and Woodgate, R. A. Seasonal and interannual variability of pan-Arctic surface mixed layer properties from 1979 to 2012 from hydrographic data, and the dominance of stratification for multiyear mixed layer depth shoaling. *Progress in Oceanography*. 2015, 134, p. 19–53. <https://doi.org/10.1016/j.pocean.2014.12.005>.
6. Sirevaag, A., De la Rosa, S., Nicolaus, I. F. M., Tjernström, M. and McPhee, M. G. Mixing, heat fluxes and heat content evolution of the Arctic Ocean mixed layer. *Ocean Science*. 2011, 7 (3), p. 335–349. <https://doi.org/10.5194/os-7-335-2011>.
7. Steele, M., Ermold, W. and Zhang, J. Modeling the formation and fate of the near-surface temperature maximum in the Canadian Basin of the Arctic Ocean. *Journal of Geophysical Research: Oceans*. 2011, 116 (C11). <https://doi.org/10.1029/2010JC006803>.
8. Polyakov, I. V., Pnyushkov, A. V., Rember, R., Padman, L., Carmack, E. C. and Jackson, J. M. Winter Convection Transports Atlantic Water Heat to the Surface Layer in the Eastern Arctic Ocean. *Journal of Physical Oceanography*. 2013, 43 (10), p. 2142–2155. <https://doi.org/10.1175/JPO-D-12-0169.1>.
9. Shimada, K. et al. Pacific Ocean inflow: Influence on catastrophic reduction of sea ice cover in the Arctic Ocean. *Geophysical Research Letters*. 2006, 33, L08605. <https://doi.org/10.1029/2005GL025624>.
10. Carmack E. C. et al. Freshwater and its role in the Arctic Marine System: Sources, disposition, storage, export, and physical and biogeochemical consequences in the Arctic and global oceans. *Journal of Geophysical Research: Biogeosciences*. 2015, 121 (3), p. 675–717. <https://doi.org/10.1002/2015JG003140>.
11. Rosenblum, E., Fajber, R., Stroeve, J. C., Gille, S. T., Tremblay, L. B. and Carmack, E. C. Surface Salinity Under Transitioning Ice Cover in the Canada Basin: Climate Model Biases Linked to Vertical Distribution of Fresh Water. *Geophysical Research Letters*. 2021, 48 (21): e2021GL094739. <https://doi.org/10.1029/2021GL094739>.
12. Kimura, S., Kikuchi, T., Fujiwara, A., Mahoney, A., Eicken, H. and Goda, T. Sea-ice motion and oceanographic data from the Beaufort Sea to the Chukchi Borderland in March–December 2020. *Polar*

Data Journal. 2021, 5, p. 60–68. <https://doi.org/10.20575/00000027>.

13. Hill, V. J., Light, B., Steele, M., Zimmerman, R. C. Light Availability and Phytoplankton Growth Beneath Arctic Sea Ice: Integrating Observations and Modeling. *Journal of Geophysical Research: Oceans*. 2018, 123 (5), p. 3651–3667. <https://doi.org/10.1029/2017JC013617>.

#### **Data Citations**

Kimura Satoshi, Kikuchi Takashi, Fujiwara Amane, Jones Joshua, Kaku Masahiro, & Kensuke Watari. (2023). Sea-ice motion and oceanographic data from the Beaufort Sea to the Chukchi Borderland in March–October, 2022 (Version ICEX2022) [Data set]. Zenodo. <https://doi.org/10.5281/zenodo.7812496>.